Chapter 2

Development and Applications of Upconversion Nanoparticle in Biosensing

Liuen Liang, Andrei V. Zvyagin and Run Zhang

2.1. Introduction

Biochemical sensing is of growing importance in healthcare applications due to the capability of early detection of disease biomarkers as well as real-time and continuous monitoring of target analytes in complex biological activities. Among the various sensing techniques, optical sensing using fluorescent or luminescent biosensors for the detection of trace amounts of analytes is getting increasing attention because of its simplicity, high sensitivity, and versatility in obtaining diverse information in biological systems. The applications of these optical biosensors in non-invasive detection of analytes in live cells, tissues, and animals are also speeding up with the supports from rapid development of optical microscopy.

In light of that, the use of fluorescence receptors such as organic dyes, transition metal complexes, rare-earth chelates, and quantum dots has attracted considerable interest in the sensing research community. However, *in vitro* and *in vivo* assays of biomarkers remains challenges due to high activities of analytes and lacks of effective detection approaches. In particular, development of fluorescent and/or luminescent biosensors for the detection of highly reactive biomolecules in

Run Zhang
School of Chemical Engineering, University of Science and Technology Liaoning, 185 Qianshan Zhong Road, Anshan 114044, P. R. China
Australian Institute for Bioengineering and Nanotechnology, The University of Queensland, St Lucia, QLD, 4072, Australia

complicated biological conditions is highly demanded. Typically, desirable optical biosensors must: (i) Fast respond to biomolecules, giving changes in fluorescence/luminescence signals; (ii) Be highly sensitive and selective towards targets; (iii) Discriminate the background autofluorescence from biological samples; (iv) Be highly photostable, ensuring their long-term *in viv*o monitoring of biological activities; (v) Possess low toxicity and exert no phototoxicity to live bodies during detection.

These criteria are satisfied when using near-infrared (NIR)-excitable nanoparticles, where the luminescent nanoparticles can be excited by NIR light to elicit the photoluminescence for biological analysis. NIR light falls into the biological transparency window (700-1300 nm), it penetrates deeper and excites considerably less autofluorescence and exerts less phototoxicity compared to UV and visible light [1]. Considering that, upconversion nanoparticles are ideal candidate for development of nanosensors in biological applications as they exhibit high photostability, great emission intensity, and most importantly, being exciting by the NIR irradiation.

UCNPs are a type of inorganic nanocrystals comprised of a host matrix to embed the lanthanide dopants, absorbing dopants to harvest NIR light, and emitting dopants to produce the upconversion photoluminescence. The upconversion refers to a non-linear optical process in which the nanoparticle sequentially absorbs two or more low-energy NIR photon and emits a high-energy photon of short wavelength. In contrast with multiphoton process used to excite organic fluorescent dyes or other photoluminescent nanoparticles, the absorption of photons in UCNPs occurs via a real energy level and the upconversion process is several orders of magnitude more efficient, allowing the nanoparticles to be excited at low excitation energy (typically, 1-1000 W/cm^2) [2]. The upconversion emission originates from this energy absorption and transfer process among lanthanide dopants in the host matrix. Therefore, the spectral properties and emission efficiency of UCNPs are largely determined by the selection of UCNP host matrix, the dopant ions, and their doping level. For example, Er^{3+} doped $NaYF_4$:Yb nanocrystals brings about mainly green (Em = 540 nm) and red emission (Em = 655 nm), while Tm^{3+} doped $NaYF_4$: Yb results in dominant blue (Em = 450, 475 nm) and NIR emission (Em = 800 nm) (Fig. 2.1).

The low energy NIR excitation together with the tunable upconversion emission of UCNPs have found them a variety of applications in

biomedicine, such as high contrast bioimaging [3, 4], drug delivery [5], photodynamic therapy [4-7], and photothermal therapy [8]. These outstanding properties stemming from the upconversion photoluminescence have also be recognized for enormous potential in biosensing [9, 10]. In this chapter, we present a comprehensive review that covers the main aspects of the development and applications of UCNP-based biosensors, including discussion of optical merits of UCNPs in the context of biosensing, nanoparticle synthesis strategies, design of UCNP nanosensors, and examples of applications of UCNP-based biosensors.

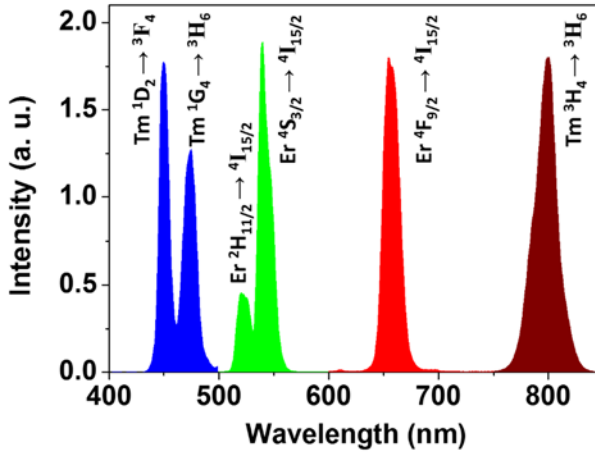

Fig. 2.1. Luminescence emission of UCNPs, blue (Em = 450, 475 nm) and NIR emission (Em = 800 nm) from Tm^{3+} doped nanocrystal, and green (Em = 540 nm) and red emission (Em = 655 nm) from Er^{3+} doped nanocrystal.

2.2. Optical Properties of UCNPs

The upconversion photoluminescence process takes place via a combination of several complex optical pathways, such as ground state absorption, excited state absorption, and energy transfer [11]. In a simplified upconversion process, an incoming NIR photon pumps the absorbing ion (typically Yb^{3+}) from its ground state to an excited state from which a non-radiative energy transferred to the neighboring emitting ion (typically Er^{3+}, Tm^{3+}, and Ho^{3+}) takes place, and promotes it to an intermediate excited state. Another incoming NIR photon stimulates the sequential process of the non-radiative energy transfer,

resulting in the same absorbing ion being transferred to the higher excited state. Following the energy transfer, the emitting ions relax to their ground state, while the activator ion at its higher excited state undergoes non-radiative relaxation to the lower energy states, followed by radiative decays with characteristic upconversion emission and eventually returning to its ground state (Fig. 2.2). This unique photoluminescence process ensure UCNPs with many excellent optical properties for biosensing. In this section, a brief description of the optical properties of UCNPs is presented.

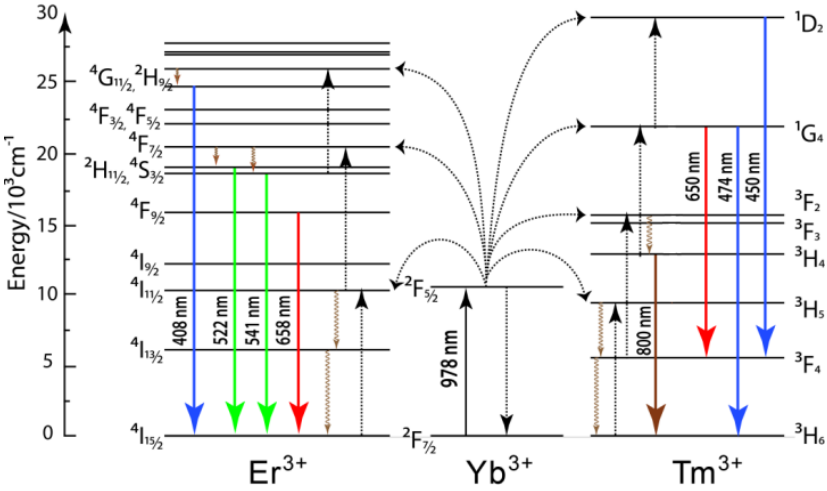

Fig. 2.2. Under NIR laser irradiation, energy transfer mechanisms illustrating upconversion energy transfer processes in Yb^{3+}, Er^{3+}/Tm^{3+} co-doped UCNPs.

2.2.1. Large anti-Stokes Shift and Narrow Multicolour Emission

Generally, fluorescence emitters rely on a single photon excitation occurring in UV or visible spectral range to produce emission with the lower photon energies, the process known as Stokes emission. In contrast, upconversion nanoparticles sequentially absorb two or more low-energy photons at the higher wavelength (*e. g.* 980 nm) producing anti-Stokes emission at the shorter wavelength. This multiphoton process results in a large anti-Stokes shift (up to 500 nm) between the excitation and emission wavelengths, allowing more efficient and easy separation of the photoluminescence and excitation light. Additionally, the

emission peaks of UCNPs are narrow-band in comparison with the conventional photoluminescent nanoparticles, with the emission bandwidths being typically ~20 nm. Meanwhile, UCNPs are characterized by a unique set of distinguishable emission peaks. These multicolour peaks are narrow and featured, usually excited simultaneously using a single NIR continuous-wave excitation source. Hence, the multicolour property of UCNPs is beneficial in the design of ratiometric biosensors, where one emission peak is used as a constant reference and a second emission is modulated by the analyte. On the other hand, the multiple emission of UCNPs can also be harnessed for multiplexed detection of different analytes by using the well-separated emissions of UCNPs. This technology allows for simultaneous identification and quantifications of multiple distinctive analytes in complex environment [12]. For example, Rantanen and co-workers fabricated a multiplexed detector for DNA by using the two distinct emission bands of UCNPs ($NaYF_4$:Yb,Er) [13]. In their design, UCNPs were coupled with two different capture oligonucleotides, which would specifically detect the target DNA label with Alexa Fluor 546 or Alex Fluor 700. Upon NIR excitation, the green and red emissions from UCNPs were selectively absorbed by the two fluorophore labels, leading to excited emission of the acceptors at 600 nm and 740 nm, respectively. DNA hybridization between different strands was therefore detected simultaneously without mutual interference [13].

2.2.2. Tuneable Upconversion Luminescence

The capability of manipulating the output colour is another fascinating property of UCNPs, especially when the nanoparticles are used as a donor in the luminescence resonance energy transfer (LRET)-mediated sensing application. LRET is a non-radiative energy transfer process happening between an energy transfer donor and an energy transfer acceptor in a restricted distance (1-10 nm). The on/off energy transfer between UCNP (donor) and fluorophore (acceptor) can be activated or deactivated upon the recognition of the analytes, which provides an effective and simple way for the development of UCNPs-based biosensors. Based on this strategy, a variety of sensing platforms have recently been developed for bioanalysis with improved sensitivity and efficiency [14]. To obtain the high sensitivity in detection, it is critical to choose a good LRET pair with emission of the donor (UCNPs) overlapping well with the absorption band of the acceptor. To this end, UCNPs can act as a flexible donor to provide the diverse selection of

emission wavelengths and intensities to the desired receptors. The emission color and intensities of UCNPs is tuneable by various strategies, encompassing varying the host lattices [15], controlling the doping composition [16] and concentration [17], and exploiting the core-shell structure [18], which have been extensively reviewed [19]. These emission profiles of UCNPs also provide opportunities for engineering UCNPs-based optical biosensors, where UCNPs serve as the signaling moiety to report the levels of specific analyte.

2.2.3. Non-invasive and Sensitive Bioassay in Deep Tissues

Capabilities for non-invasive and high-sensitive detection of specific biomolecules in deep tissue is another compelling reason for the development of UCNPs-based nanosensors. In optical biosensing, light travelling through biological tissues undergoes multiple events of absorption and scattering that will contribute to the attenuation of the light. The absorption is mainly caused by biomolecules such as haemoglobin, oxyhaemoglobin in the blood – in UV/visible part of the spectrum; and water – in the NIR. The scattering process takes place on the boundaries between optical interfaces, being more efficient on high refractive-index structures, including lipids, melanin, *etc*. This attenuation effect is minimal when using light at the wavelength range from 700 nm to 1300 nm, a biological tissue transparency window [1]. The characteristic excitation of a particular type of UCNPs, Tm-doped UCNPs at 980 nm and its NIR emission at ~800 nm fall into this region, minimizing the effects of absorption and scattering, are thus considered advantageous for deep-tissue sensing.

Additionally, the autofluorescence from biological samples is greatly eliminated due to the NIR excitation. As a result, a high contrast of UCNPs and low autofluorescence signal can be detected in a crowded background of biological samples. For example, Li's group exploited the ratiometric emission of $NaYF_4$:Yb,Er,Tm at 800 nm to 660 nm to design an efficient and highly sensitive probe for the detection of methylmercury ions ($MeHg^+$) in living animal [20]. In this study, UCNPs were surface modified with a NIR dye heptamethine cyanine dye (hCy7'), which was responsive to $MeHg^+$ and thereby changed its absorption maxima from 670 nm to 845 nm. In presence of $MeHg^+$, energy transfer between hCy7' and UCNPs was increased, resulting in the decrease in NIR emission of UCNPs to be detected *in vivo* by upconversion bioimaging [20].

2.2.4. Superb Photostability

A single fluorescent dye molecule (*e.g.* Rhodamine 6G) typically survives about 1 million excitation-emission cycles, followed by transition to a triplet metastable state from where it reacts with neighboring molecules and undergoes an irreversible transition to the dark state, leading to the cessation of its fluorescence. Fluorescence intermittency or blinking is another consideration for bioimaging *in vivo*. Recent studies on the photostability of a single UCNP showed virtually no photobleaching of the particle during the 1 h of continuous illumination with a 10 mW 980 nm laser [21]. Additionally, no photoblinking of UCNPs at timescales down to 1 ms was observed [21], making this photoluminescence material attractive as optical contrast probe with real-time monitoring and long-term tracking capabilities. For instance, Lai *et al.* developed a UCNPs-based nanohybrid as a drug delivery vehicle as well as a real-time monitoring sensor of drug release within the tested 24 hours in live cells [22]. The multicolor UCNPs was coated with a mesoporous silica to allow the loading of chemotherapeutic drugs in the nanohybrid. As the result of energy transfer from UCNPs to drugs, the emission in UV-vis range was quenched, while the NIR emission was retained. The release of drugs led to the reduction in energy transfer, and thus the emission in UV-vis range was switched on. By virtue of the superb photostability of UCNPs, the drug release from this drug carrier was then monitored by the ratiometric signal of UV-vis and NIR emission of UCNPs [22].

2.3. Development of UCNP-based Biosensors

Upconversion nanoparticle itself is inert to the surrounding microenvironment, while the UCNPs-based nanosensors can be designed by integrating responsive molecules, such as molecular chemosensors with this upconversion nanomaterial. Two different sensing mechanisms have been reported in the applications of UCNPs-based biosensors, namely, inner filter effect and luminescence resonance energy transfer (LRET). In the first case, the emission of UCNPs is quenched due to re-absorption of the emission light from UCNPs by the molecules existing in the detection system. Analytes at different concentration exert a strong or an insignificant filter effect on the luminescence of UCNP, thereby giving an indication of the quantity of analytes [23-28].

LRET is a process in which energy is transferred non-radioactively from an excited donor (UCNP) to an acceptor molecular. LRET requires essentially the emission band of UCNPs overlapping well with the absorption band of the acceptor molecular and the LRET-pair (donor-acceptor) being placed in close proximity to one another (1-10 nm). Therefore, the sensing of responsive nanosensors are determined by the energy transfer efficiency, which are normally modulated either by spectrometric overlapping or changing the distance between the LRET-pair (Fig. 2.3). Fig. 2.3 (a) illustrates the design of UCNPs nanosensor based on the spectrometric overlapping strategy. In the presence of analyte, the absorption spectrum of acceptor is changed, followed by switching on the emission of UCNPs due to the elimination of LRET process. The LRET efficiency is highly dependent on the distance between the donor and acceptor, and therefore UCNPs-based nanosensors can also be designed by manipulating the distance between LRET-pair, which is presented in Fig. 2.3 (b) and (c). On the basis of these two LRET strategies, a myriad of UCNP biosensors have been developed employing the LRET mechanisms to probe a variety of delicate biological processes [14].

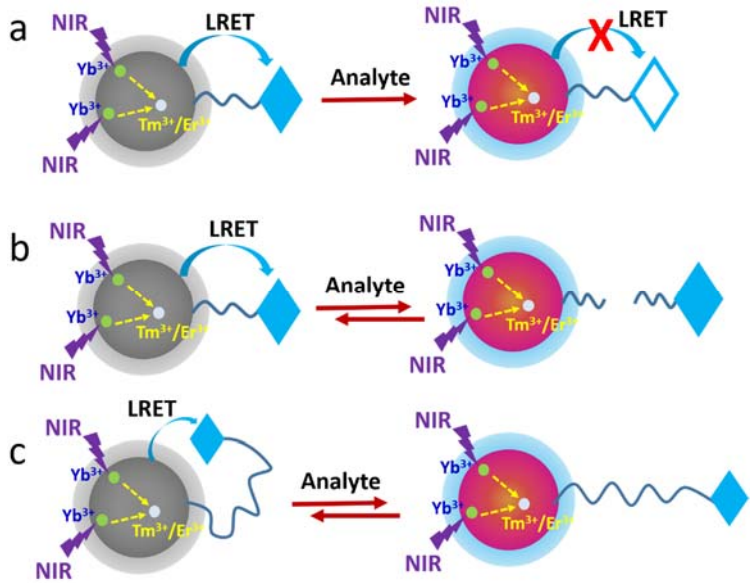

Fig. 2.3. Schematic diagram of the principles of LRET-based UCNPs nanosensors for the detection of analytes. (a) Spectra overlapping between LRET-pair; (b), (c) distance variation between LRET-pair.

In both sensing design approaches (inner filter effect and LRET), it is prerequisite to obtain UCNPs with high luminescence efficiency in order to achieve highly sensitive implementation of UCNP nanosensors. The fabrication of UCNP-donor nanohybrid is also critical to manipulate LRET process for the detection of different analytes. In the following section, the preparation approaches for high-quality UCNPs are summarized, followed by the fabrication strategies for development of UCNP sensing platforms.

2.3.1. Synthesis of UCNPs

Among various types of host materials, lanthanide (Ln) fluorides, such as LnF_3, LnOF, and MLnFn (M = Li, Na, K or Ba; n = 4 or 5) are regarded as ideal host matrices to produce efficient upconversion nanocrystals. Considering that, a number of synthesis methods have been developed to prepare lanthanide fluoride-based UCNPs with controlled size, shape, crystalline phase, and composition that presents desirable physiochemical properties for their potential applications. The most commonly used methods for the synthesis of UCNPs are thermal decomposition, hydro(solvo)thermal synthesis, and coprecipitation, which are described below.

2.3.1.1. Thermal Decomposition

Thermal decomposition is a well-established method for the synthesis of monodispersed UCNPs with uniformed shape, tailored size and single crystal structure. This strategy is based on the decomposition of organometallic precursors in the presence of organic solvents (e.g. 1-octadecane, ODE) and surfactants (*e. g.* oleic acid, OA, and oleylamine, OM). The commonly used precursors include metallic or lanthanide trifluoroacetate, lanthanide oleates, lanthanide acetates, and lanthanide chlorides. The surfactants usually contain a functional group, including -COOH, and $-NH_2$, to cap the surface of UCNPs for controlling their growth and a long hydrocarbon chain to assist their dispersion in organic solvents.

In general, the synthetic process is conducted at elevated temperature (250-330 °C) in an oxygen-free and anhydrous environment, wherein the precursors decompose to form the nucleus for a particle to grow on. This method was introduced by Yan and co-workers on the preparation of triangular LaF_3 nanoplates [29], and was later improved as a broadly

applicable route to produce UCNPs of high quality and narrow size distribution. Various sizes and shapes of UCNPs have been produced by tailoring the experimental parameters, including the reaction temperature, reaction time, nature and concentration of solvents, and the concentration of reagents. Another refined approach was reported by Li and co-worker for the preparation of β-$NaYF_4$:Yb,Er/Tm UCNPs [30]. Their method was demonstrated to be user-friendly in minimizing the use of fluoride reactions and decreasing the amount of toxic by-products generated at high temperature [30].

2.3.1.2. Hydro(solvo)thermal Synthesis

Hydro(solvo)thermal method is performed with the assistance of high temperature and pressure to dissolve solid reactants as well as to speed up the reaction. The possible advantages of this technique are the relatively lower reaction temperature, high-quality crystalline phase of the obtained nanoparticles, and excellent control over the particle size and shape. The main disadvantages are the adoption of specialized reaction vessels (Teflon-lined autoclave) and inability to monitor the particle growth. In a typical process, lanthanide precursors (such as lanthanide nitrites, chlorides, and oxides) and fluoride precursors (such as HF, NH_4F, NH_4HF_2, NaF, and KF) and surfactants are mixed in aqueous solution and placed in an autoclave, then sealed and heated at a temperature between 160 °C and 220 °C. Morphologies of the UCNP product can easily be tuned by varying the reactant concentration, reaction temperature, reaction time, and pH of the solution. This method was firstly reported by Li's group on the synthesis of $NaYF_4$, YF_3, LaF_3 and YbF_3 nanocrystals [31]. Another example of the hydro(solvo)thermal synthesis was reported by Zhao and co-workers to generate monodispersed β-$NaYF_4$ with various morphologies, such as nanorods, nanotubes, and flower-patterned nanodisks [32].

2.3.1.3. Coprecipitation

Coprecipitation approach is the most convenient and simplest way to prepare $NaYF_4$ UCNPs, since no costly equipment, complex procedures, and stringent reaction conditions are required for this synthesis. In a typical example, ethylenediaminetetraacetic acid (EDTA) was used as a chelate agent to form a lanthanide-EDTA complex, followed by a rapid injection of this complex to a vigorously stirred NaF solution [33]. This process was helpful in forming a homogenous nucleus for subsequent

growth of nanoparticles. The particle size can be effectively controlled from 37 nm to 166 nm by adjusting the molar ratio of EDTA to lanthanide salts [33]. Normally, α-$NaYF_4$ UCNPs obtained using this method display low photoluminescent yield. In view of that, a post-treatment by annealing is required to drive transition of the particles from cubic to hexagonal phase, which results in the brighter UCNPs [33]. Haase and co-workers have demonstrated successful production of water-dispersible β-$NaYF_4$ UCNPs without the need of the calcination step [2]. Besides the use of EDTA, other surface ligands, such as polyethylenimine (PEI) [32] and polyvinylpyrrolidone [34] were also employed to control the nanoparticle growth and yielded nanoparticles capped with these polymers.

2.3.2. Fabrication of UCNPs-based Sensing Platforms

The hydrophilicity and stable dispersity in biological conditions are the prerequisite for nanoparticles to be used in bioassays. However, UCNPs prepared by the methods described above are generally hydrophobic owing to the hydrophobic nature of the capping reagents (*e.g.* OA or OM), which hampers their application in biosensing. In order to transfer these hydrophobic UCNPs into hydrophilic, a number of surface modification methods have been developed, including ligand exchange [35, 36], ligand oxidation [37-39], ligand removal [40, 41], ligand attraction [42, 43], layer-by-layer assembly [44, 45], and surface silanization [46]. These surface engineering methods not only render UCNPs water solubility, but also endow UCNPs with reactive groups for subsequent conjugation to responsive molecules for development the UCNP-based nanosensors [47-49].

A successful implementation of UCNP nanosensors heavily relies on the responsive recognition molecules. Therefore, the integration of recognition components with the UCNP-sensing system is crucial for the development of UCNPs-based biosensors. For the UCNP sensors in forms of films or beads, UCNPs were mixed with detection molecules in a film matrix (*e. g*. polystyrene), where the detection probe molecules exert an effect on upconverted emission of UCNPs in response to analytes [25, 26]. In this case, LRET between UCNP and responsive probe molecules is unlikely to occur to a substantial extent due to the fact that the distance between donor and acceptor are far above the critical LRET (typically < 10 nm). To fabricate UCNP nanosensors based on LRET, efforts were made to couple recognition agents with UCNP

within the LRET distance. To date, the established methods for combining UCNPs with recognition agents include physical adsorption, coordination bond, covalent conjugation, and silica encapsulation (Fig. 2.4).

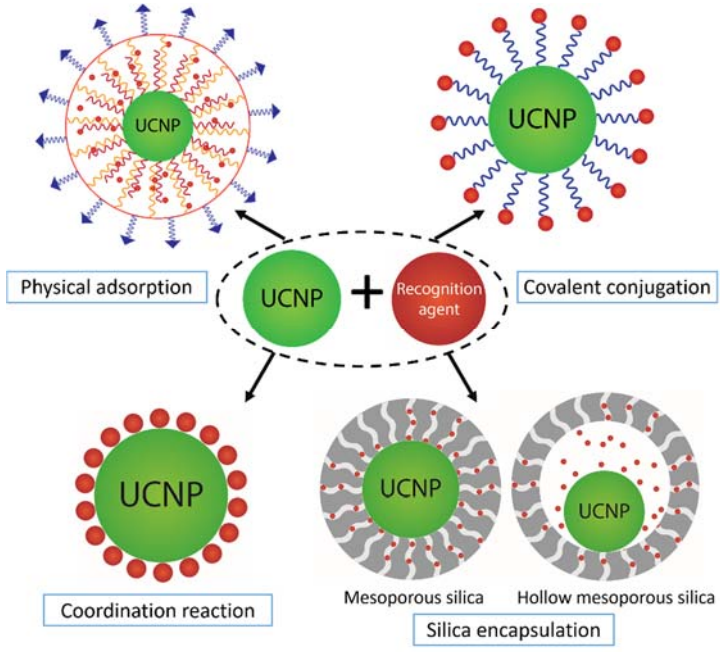

Fig. 2.4. Schematic illustrations of the four strategies for integrating UCNP with recognition agents.

2.3.2.1. Physical Adsorption

In physical adsorption strategy, UCNPs and recognition agents are generally assembled via the hydrophobic interaction or electrostatic attraction. UCNPs prepared by the aforementioned methods are normally capped with a layer of OA, which can facilitate the direct binding of some hydrophobic molecules to UCNPs. For example, Zhang et al. reported the attachment of Cu^{2+} fluorescence sensing molecules, RB-hydrazine, to UCNP surface via the hydrophobic interaction with the OA layer [50]. The hydrophobic arms of some amphiphilic polymers are normally attached to UCNP surface via hydrophobic interaction with UCNP surface ligands, creating a hydrophobic network for storage of

hydrophobic recognition agents. For example, Yao and co-workers described the loading of a CN^- reactive iridium (III) complex to amphiphilic block polymer coated UCNP, wherein the iridium complex was accommodated in a hydrophobic layer created by the interaction between hydrophobic units of the polymer and oleic acid [51]. In another report, Ding and co-workers modified UCNP with a cyclic oligosaccharide macromolecule γ-cyclodextrin (CD), which served as a doughnut-shaped cavity allowing for loading of both oleate ligands of UCNP and sensing molecules of Rhodamine B derivative [52]. On the other hand, physical adsorption can also make use of the electrostatic interaction between species with opposite charges to deposit recognition molecules on a charged surface of UCNP. For example, negatively charged graphene oxide (GO) nanosheets can be loaded on to positive charged PEI-coated UCNPs [53]. In analogy, positively charged Zn^{2+}-responsive compound was assembled onto polyacrylic acid (PAA)-modified UCNPs (negatively charged) through electrostatic attraction [54].

2.3.2.2. Coordination Bond

Because of the strong coordination capability of abundant lanthanide ions on the UCNPs surface, recognition molecules with functional groups, such as -COOH, $-NH_2$, and -OH, can be directly immobilized on UCNPs surface via coordination interaction. The coordination is conducted by replacing the original surface capping ligands with the new binding molecules that possess stronger coordination ability toward lanthanide ions. Usually, the ligand exchange reaction involves one or two steps. In on-step method, UCNPs are mixed with excess of new ligands under ultrasonication [55-57]. In two-step processes, surface ligands of UCNP are firstly removed by protonation with HCl at pH 4 [41] or treatment with nitrosonium tetrafluoroborate [36] or tetramethylammonium hydroxide [58], yielding ligand-free UCNP for subsequent attachment of new capping ligands. For example, Liu's group reported the removal of OA on UCNP with substantial amount of acidic ethanol (pH = 1), followed by tagging a Ca^{2+}-sensitive receptor on UCNP to generate a LRET-based nanosensor for Ca^{2+} detection [59].

2.3.2.3. Covalent Coupling

Compared to the physical methods, covalent conjugation between recognition molecules and UCNPs is sufficiently strong to secure the

detection reagents remaining in the nanoplatform during application in biological systems. Also, such robust binding is important for the development of UCNP-LRET based sensors, when detachment of recognition molecules is undesirable and will result in a loss of sensing efficiency. In this method, the attachment of recognition molecules to UCNP is generally achieved by cross-linking between carboxylic and amine groups on these two entities. For example, Kumar and Zhang reported the covalent conjugation of amine-containing DNA strand to carboxylic group functionalized UCNP via the carbodiimide coupling reaction [60]. This method presented a versatile strategy for binding amine-containing DNA or aptamers to UCNPs, which are also exploited by other groups [61-63]. Alternatively, recognition molecules with silanol groups can hydrolyze on the surface of silica-coated UCNPs to obtain the covalently linked UCNP-sensing complex [64].

2.3.2.4. Silica Encapsulation

Silica-coating is one of the most popular methods to endow UCNP with aqueous solubility and stability in physiological environments. In an attempt to use the silica-UCNP as delivery vehicles, efforts have been devoted to grow a mesoporous silica ($mSiO_2$) shell or hollow mesoporous silica ($hmSiO_2$) on UCNP. The silica shell on the outer layer of the particle can offer a large storage space for loading recognition agents in the mesoporous channels. A number of biosensors have been developed by incorporating recognition molecules in UCNP@$mSiO_2$ for the detection of hydrogen sulfide [65], Cu^{2+} [66], and pH [67]. A cavity between UCNP and mesoporous silica layer in UCNP@$hmSiO_2$ further advances the design in enabling much higher loading level of recognition agents [68, 69], as compared with UCNP@$mSiO_2$. In addition, the surface of silica is easily conjugated with functional groups, such as amine, thiols, and carboxyl groups, which in turn facilitate the conjugation of biomolecules or targeting ligands to UCNPs.

2.4. Applications of UCNPs in Biosensing

As a novel class of luminophore, UCNPs have been demonstrated its feasibility in the development of multiple *in vitro*, *ex vivo*, and *in vivo* biosensing models as the energy donor [9, 14]. The following section summarized some of the recent studies on development and applications

of UCNPs-based biosensors, broadly grouped into sensing of ions, biomolecules, and gas molecules.

2.4.1. UCNPs Nanosensors for the Detection of Ions

Hazardous ions, such as CN^- and Hg^+ are known as extremely toxic chemicals that can cause serious problems to the environment and health. Selective detection and bioimaging of these ions are of great importance for the biological systems. On the other hand, metal ions such as Fe^{3+}, Cu^{2+}, Zn^{2+}, Na^+, K^+, and Ca^{2+} are essential trace elements involved in many biological activities. Imbalance of these metal ions are implicated in various disorders for life processes [27, 28, 50, 52, 54]. Monitoring the level of these ions is thus significant for physiological concerns.

In this aspect, by exploiting the LRET-based mechanism, the prepared UCNP nanosensors provide particular useful tools for highly sensitive and selective detection of these ions *in vitro* and *in vivo*. Here, the ions responsive molecules are typically integrated with UCNPs in a nanocomplex, where the upconversion emission of UCNPs dominates the energy transfer efficiency from UCNPs to responsive molecules. This energy transfer can also be manipulated by a specific recognition process between responsive molecules and analyte [10]. The inhibition and promotion of energy transfer from UCNP to indicating probes will lead to changes in luminescent intensity of UCNP, thereby providing the evaluation of concentrations of target ions [70].

In a typical example, Li's group reported a UCNPs-based ratiometric luminescence probe for sensing of CN^-. The responsive chromophoric iridium (III) complex was employed for manipulating the green and red emissions of UCNPs [71]. As the result of specific reaction between iridium (III) complex and CN^-, the energy transfer from UCNPs to iridium (III) complex was diminished, followed by the recovery of green emission of UCNPs (Fig. 2.5) [71]. This UCNPs nanosensor exhibited low detection limit of 0.18 μM for CN^- in the aqueous solutions, however was not applicable in pure water due to hydrophobic nature of the iridium (III) complex [71]. Further study conducted by the same group showed that the water solubility was significantly improved when coating the UCNPs surface with amphiphilic block-polymers. The CN^--reactive iridium (III) complex, $(ppy)_2Ir(dmpp)]PF_6$, was loaded to the formed hydrophobic layer for the detection of CN^- in pure water [51].

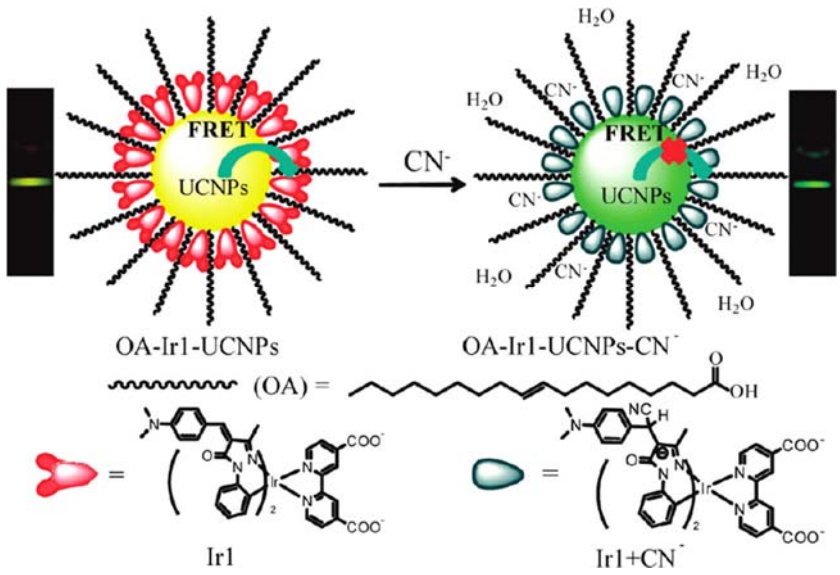

Fig. 2.5. Recognition mechanism and the LRET process of Ir1-UCNPs towards CN^-. Reprinted with permission from ref. [71].
Copyright 2011 American Chemical Society.

In another work, Li's group fabricated a Hg^{2+} sensor by assembling a water soluble Hg^{2+} probe ruthernium complex N719 directly to UCNP ($NaYF_4$:Yb,Er,Tm) via ligand exchange approach (Fig. 2.6) [55]. Upon interaction with Hg^{2+}, maximum absorption of N719 shifted from 541 to 485 nm, resulting in the decrease in spectral overlap between green emission of UCNPs and the absorption of N719. Therefore, the green emission of UCNPs was recovered, and the Hg^{2+} levels was determined [55]. This designed N719-UCNP nanosensor has also shown to be applicable in monitoring the distribution of Hg^{2+} in living cells by upconversion luminescence imaging [55].

2.4.2. UCNPs Nanosensors for the Detection of Biomolecules

Molecular recognition and specific interaction between biotin and avidin, antibody and antigen, aptamer and receptor, and molecular binding via enzyme reaction and DNA hybridization have provided reliable and versatile routes for the fabrication of biosensors with sensitivity and specificity. These strong interactions can also be utilized to manipulate the interaction between UCNPs and analytes for detection

of molecular analytes at the nanoscale level by triggering or inhibiting the energy transfer process.

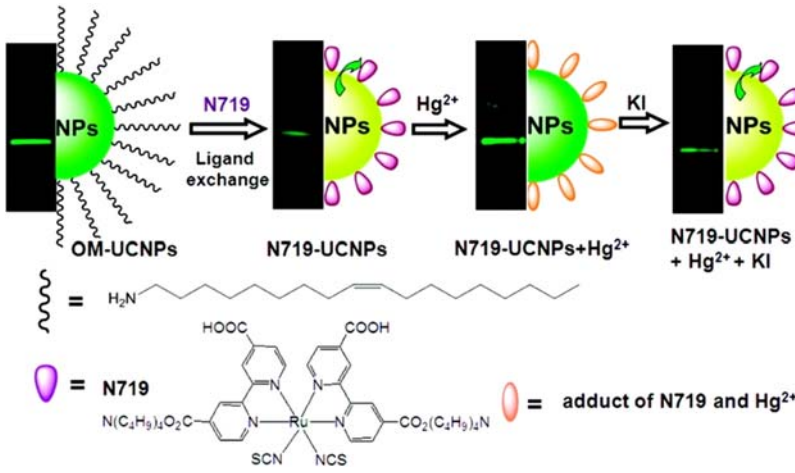

Fig. 2.6. Schematic illustration of preparation of N719-modified $NaYF_4$:Yb,Er,Tm and its sensing functionality. Reprinted with permission from ref. [55]. *Copyright 2011 American Chemical Society.*

2.4.2.1. Application of UCNPs in DNA Detection

DNA hybridization, the complementary interaction between probe DNA and sample DNA, is a major technique for the detection of genetic disease sequences. The DNA hybridization can be monitored by developing UCNPs-based sensors, where the sample DNA can be detected through ratiometric changes in luminescence emission of UCNPs. Based on this approach, Zhang and co-workers reported a simple designed UCNPs nanosensors for sensing of DNA [72]. This UCNP nanosensor was developed by conjugating capture oligonucleotide to green-emitting UCNPs, and labeling the reporter oligonucleotide with green-absorbing fluorescent dye TAMRA (Fig. 2.7 (a)) [72]. In presence of target oligonucleotide, the hybridization occurred, leading to the upconverted green emission being quenched by energy transfer between UCNP and TAMRA [72].

In an alternative way, Zhang and co-workers presented the use of an intercalating dye SYBR Green I as a fluorescent indicator to bind to the hybridized double strands of DNA [61]. After hybridization, SYBR

Green I was intercalated between target nucleotide and UCNP conjugated probe nucleotide (Fig. 2.7 (b)) [61]. Under NIR illumination, the green emission from UCNP was transferred to SYBR Green I, therefore, the DNA detection can be achieved by recording the enhancement in emission of SYBR Green I and decreased luminescence of UCNP [61]. These two schemes have also be applied to the LRET detections of DNA in other studies [13, 73, 74].

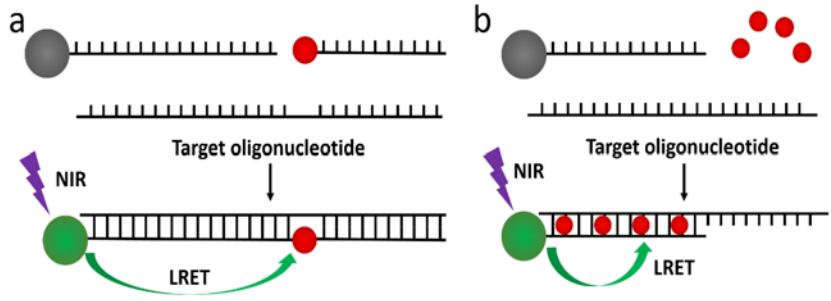

Fig. 2.7. Schematic illustration of design of UCNP-LRET oligonucleotide sensors based on the hybridization of DNA.

In design of LRET based UCNP sensors, the hybridization process of DNA can also be used together with the special interaction between graphene oxide (GO) and DNA. Single-stranded DNA (ssDNA) can be firmly attached to GO surface via the nucleobases-graphene binding, while double-stranded DNA (dsDNA) showed weak attachment towards GO. The changes on the binding affinity between ssDNA and dsDNA to GO are therefore adopted to discriminate DNA sequences. Kanaras, et al. exploited the LRET between UCNPs and GO and the hybridization of DNA to prepare a sensitive DNA sensor [62]. UCNPs were coated with a silica layer of 11 nm, and further attached with ssDNA via covalent conjugation (Fig. 2.8). When the nanocomplex interacted with GO templates, the spectral overlap between fluorescence emission of UCNP and the absorption of GO resulted in quenching the emission of UCNPs (Fig. 2.8). However, in the presence of the complementary DNA strands, the dsDNAs formed by hybridization, leading to the detachment of UCNP from GO and therefore the reduced quenching effect of GO to UCNP. The detection limit of this new method was shown to be 5 pM, demonstrating the high sensitivity of the developed sensors [62].

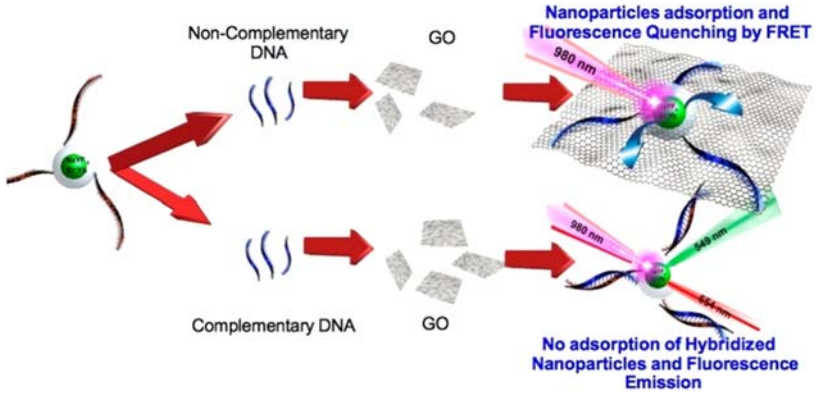

Fig. 2.8. Schematic illustration of the DNA sensor based on DNA hybridization and LRET between UCNP and GO. Reprinted with permission from ref. [62]. *Copyright 2015 American Chemical Society.*

2.4.2.2. Application of UCNPs in the Detection of Small Molecules, Proteins and Enzymes

Determination the levels of biomolecules, such as amino acids, proteins, and enzymes in biological samples plays a key role in understanding their physiological function in live systems, though remains challenging. Rapid development of biosensing technology makes detection of these molecules *in situ* possible. Recent studies on engineering of UCNPs-based approaches accelerates the applications of optical biosensors for the background-free detection of these molecules with high sensitivity and selectivity. Up to now, a number of UCNP sensors have been developed to detect a wide range of biomolecules, such as thrombin [75, 76], antigens [77], hemoglobin [78], adenosine triphosphate [79], cysteine/homocysteine [69], glucose [80], glutathione [81], matrix metalloproteinase [82], mycotoxins [83], siRNA [84], miroRNA [85], messenger RNA [86]. These representative studies provide paradigms for the design of UCNP-sensors in bioanalysis applications. In this section, we will present some examples of UCNPs-based optical biosensors for the quantification of proteins and enzymes.

By using UCNPs as the energy donor, and gold nanoparticle as the energy acceptor, Li and co-workers fabricated an effective LRET platform for the detection of trace amounts of avidin [44]. In their work, both UCNPs ($NaYF_4$:Yb,Er) and gold nanoparticles were conjugated with biotin, and the quantitative analysis of avidin was achieved when

UCNP and gold NPs were bridged by avidin, and luminescence of UCNPs were gradually quenched by gold NPs with increasing amounts of avidin [44]. The strategy of energy transfer from UCNPs to gold nanoparticles has also been exploited for the detection of goat anti-human IgG antibodies by Xu's group [87]. In their study, UCNP and gold NPs were conjugated to rabbit anti-goat IgG antibodies and human IgG antibodies, respectively (Fig. 2.9). Upon the addition of goat anti-human antibodies, UCNP and gold nanoparticles were linked via the sandwich-type immunoreaction, which in turn initiated the LRET between UCNP and gold NPs , thus quenching the emission from UCNP [87].

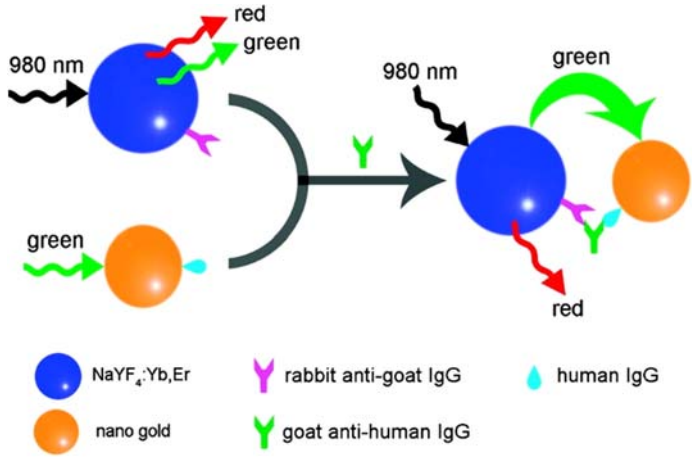

Fig. 2.9. Schematic illustration of detecting anti-human IgG antibodies using the LRET process between UCNP and gold NPs. Reprinted with permission from ref. [87]. *Copyright 2009 American Chemical Society.*

Besides graphene oxide and gold NPs, carbon nanoparticles with strong quenching ability to fluorescence have also been used to construct UCNP-based LRET sensors. The group of Pang reported the development of an aptamer biosensor for the detection of thrombin based on the LRET between UCNPs to carbon nanoparticles [79]. In their work, a thrombin aptamer was covalently conjugated to PAA modified UCNP, allowing the further binding of UCNPs to carbon NPs via π-π stacking interaction [79]. As a result, the fluorescence of UCNPs was quenched when the two NPs were brought into close proximity. In the presence of thrombin, the luminescence from UCNPs was restored due

to the released binding of carbon NPs to UCNPs, induced by the thrombin-mediated quadruplex structure formation of aptamer. Because of the strong fluorescence quenching ability and excellent biocompatibility of carbon NPs, the formed UCNP-carbon NPs biosensor demonstrated favorable sensing performance in human plasma samples [79].

2.4.3. UCNPs Nanosensors for the Detection of Gas Molecules

The determination of gases contents of oxygen, carbon dioxide, ammonia, hydrogen sulfide, and many other gases is important to correlate their roles with diseases in living systems, which in turn provide crucial information to understand their physiological and pathological functions and to develop advanced medicine for disease treatment. In this regard, the optical sensing using UCNP is particularly useful in affording the photostable upconverted luminescence in biological samples.

The first example of UCNP-based gas sensor was reported by the group of Wolfbeis. The sensor was prepared by embedding the pH sensitive probe bromothymol blue (BTB) with $NaYF_4$:Yb,Er in CO_2 permeable polystyrene film [24]. The absorption of BTB overlapped with the green and red emission of UCNP. Once CO_2 penetrated the film, the pH of the microenvironment was changed, and the absorption of BTB was decreased due to protonation, followed by the enhancement of luminescence from UCNPs. The principle of pH changes can also be applied for the development of UCNPs-based ammonia sensors [88, 89]. These optical sensors for ammonia are based on a change in either color or fluorescence of the indicator dye from transduction of pH.

It has been well-known that the transition metal complexes, such as ruthenium (II) and iridium (III) complexes are oxygen-sensitive, and can be used as the sensor for the detection of oxygen levels. More importantly, the absorption spectra of these metal complexes are well matched with the blue or green emissions of UCNPs. Taking advantages of these properties, Su's et al. presented the first integration of UCNPs with oxygen-sensing ruthenium (II) complex into one nanoplatform for oxygen sensing [64]. In a subsequent study, Wolfbeis and co-workers demonstrated the oxygen detection by using UCNPs as the nanolamp, and an iridium (III) complex as the switchable molecular probe for oxygen [26]. The absorbance of iridium complex strongly overlapped with the blue emission of UCNPs. Therefore, the NIR-excited blue

emission of UCNPs was demonstrated to be absorbed by iridium complex to generate its green-yellow luminescence, which was quenched during the sensing of oxygen [26].

Recently, Shi's group demonstrated the application of UCNPs-$[Ru(dpp)_3]^{2+}Cl_2$ systems for the diagnosis of hypoxic level in living organisms by exploiting the UCNPs-based LRET approach [68]. The nanosensor was prepared by loading oxygen-sensitive ruthenium (II) complex into the hollow cavity of UCNP@hmSiO_2, wherein the distance between UCNP donor and ruthenium acceptor was maintained to be within 10 nm (Fig. 2.10). Under NIR exposure, the energy transfer between UCNP and ruthenium (II) complex resulted in the illumination of ruthenium (II). Since the luminescence intensity of ruthenium (II) complex is oxygen dependent, the hyperoxic or hypoxic conditions in both cells and live zebrafishes were then determined by spectrometric analysis and bioimaging.

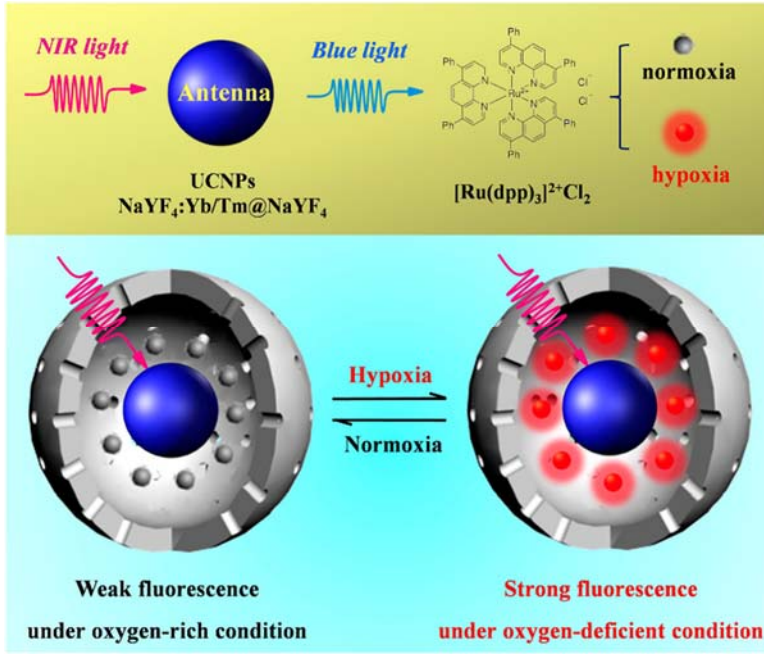

Fig. 2.10. Schematic illustration of UCNP-based oxygen nanosensor by impregnating the oxygen-responsive indicator into hollow cavity of UCNP@hmSiO_2. Reprinted with permission from ref. [68]. *Copyright 2014 American Chemical Society.*

Based on the similar LRET strategy, Liu and co-workers prepared a UCNPs nanosensor for the highly sensitive and selective detection of HS^- in living cells [65]. The UCNP sensing platform was designed by coating a mesoporous silica shell on UCNP, and immobilizing the HS^- sensitive probe merocyanine (MC) into the mesopores of the $mSiO_2$ layer. Upon the interaction of MC with HS^- to form MCSH, the absorption at ~548 nm was decreased. Therefore, the green luminescence emission from UCNPs was increased as the diminishment of energy transfer from UCNPs to dye molecules. In addition, ratiometric luminescence detection of HS^- was achieved by using the emission at 800 nm as the internal standard.

2.5. Conclusions

Research exploring the use of luminescent nanoparticles for optical sensing is driven by the increasing demands for high accuracy and sensitivity in bioassays. In this sense, the emerging upconversion nanoparticles that are illuminated by NIR light provide numerous opportunities for sensitive biological sensing, particular for the detection of biomolecules in complicated biological conditions. UCNP demonstrate remarkable optical properties, including large anti-Stokes shift, narrow emission bands, tuneable emission spectrum, and excellent photostability. These merits of UCNPs together with the flexible surface chemistry and low toxicity have made UCNPs a successful luminescent platform for the development of biosensors for the detection of ions, biomolecules, and biological gases that are summarized in this chapter.

Although great potentials of UCNPs have been widely recognized, challenges still exist in implementation of UCNPs in biosensing. First of all, small and bright UCNPs are required in the context of biological optical imaging and sensing. However, the reproducible preparation of small UCNPs with improved upconversion luminescence efficiency remains challenging. Secondly, significant quenching of upconversion emission in water solution is undesirable for their application in biological systems. Thirdly, the elaborate design of LRET UCNP sensors entails further investigation to optimize the energy transfer between UCNP and sensing probe, and to elucidate the contribution of LRET and emission-reabsorption to the sensing efficiency. Fourthly, besides the LRET, novel sensing mechanism for the design of UCNPs-based nanosensors are demanded. Lastly, applications of the designed UCNPs in addressing the practical medical problems needs to be explored. Since

this nanotechnology is progressing gradually, we can envision that more applications of UCNPs-based biosensing will be achieved in the not-too-distant future.

Acknowledgements

We wish to acknowledge the financial supports from Australian Research Council (DE170100092, DP170104749), National Health and Medical Research Council (APP1125794), and National Natural Science Foundation of China (21601076), and Russian Federation (Megagrant: 14.Z50.31.0022). This work is also partially supported by the Australian Research Council through its Centre of Excellence scheme (CE140100003).

References

[1]. P. N. Prasad, Introduction to biophotonics, *John Wiley & Sons*, 2004.
[2]. S. Heer, K. Kömpe, H. U. Güdel, M. Haase, Highly efficient multicolour upconversion emission in transparent colloids of lanthanide-doped $NaYF_4$ nanocrystals, *Advanced Materials*, 16, 2004, pp. 2102-2105.
[3]. A. Nadort, V. K. Sreenivasan, Z. Song, E. A. Grebenik, A. V. Nechaev, V. A. Semchishen, V. Y. Panchenko, A. V. Zvyagin, Quantitative imaging of single upconversion nanoparticles in biological tissue, *PloS One*, 8, 2013, e63292.
[4]. L. Liang, Y. Lu, R. Zhang, A. Care, T. A. Ortega, S. M. Deyev, Y. Qian, A. V. Zvyagin, Upconversion nanoparticles mediated deep-penetrating photodynamic therapy of KillerRed, *Acta Biomaterialia,* 51, 2017, pp. 461-470.
[5]. D. Yang, Z. Hou, Z. Cheng, C. Li, J. Lin, Current advances in lanthanide ion (Ln^{3+})-based upconversion nanomaterials for drug delivery, *Chemical Society Reviews,* 44, 2015, pp. 1416-1448.
[6]. L. Liang, A. Care, R. Zhang, Y. Lu, N. H. Packer, A. Sunna, Y. Qian, A. V. Zvyagin, Facile assembly of functional upconversion nanoparticles for targeted cancer imaging and photodynamic therapy, *ACS Applied Materials & Interfaces,* 8, 2016, pp. 11945-11953.
[7]. E. Khaydukov, K. Mironova, V. Semchishen, A. Generalova, A. Nechaev, D. Khochenkov, E. Stepanova, O. Lebedev, A. Zvyagin, S. Deyev, Riboflavin photoactivation by upconversion nanoparticles for cancer treatment, *Scientific Reports,* 2016.
[8]. L. Cheng, K. Yang, Y. Li, X. Zeng, M. Shao, S.-T. Lee, Z. Liu, Multifunctional nanoparticles for upconversion luminescence/MR

multimodal imaging and magnetically targeted photothermal therapy, *Biomaterials*, 33, 2012, pp. 2215-2222.

[9]. D. E. Achatz, R. Ali, O. S. Wolfbeis, Luminescent chemical sensing, biosensing, and screening using upconverting nanoparticles, Luminescence applied in sensor science, *Springer*, 2010, pp. 29-50.

[10]. S. Hao, G. Chen, C. Yang, Sensing using rare-earth-doped upconversion nanoparticles, *Theranostics*, 3, 2013, pp. 331-345.

[11]. A. Nadort, J. Zhao, E. M. Goldys, Lanthanide upconversion luminescence at the nanoscale: fundamentals and optical properties, *Nanoscale*, 8, 2016, pp. 13099-13130.

[12]. S. Wu, N. Duan, Z. Shi, C. Fang, Z. Wang, Simultaneous aptasensor for multiplex pathogenic bacteria detection based on multicolor upconversion nanoparticles labels, *Analytical Chemistry*, 86, 2014, pp. 3100-3107.

[13]. T. Rantanen, M. -L. Järvenpää, J. Vuojola, R. Arppe, K. Kuningas, T. Soukka, Upconverting phosphors in a dual-parameter LRET-based hybridization assay, *Analyst*, 134, 2009, pp. 1713-1716.

[14]. Q. Su, W. Feng, D. Yang, F. Li, Resonance Energy Transfer in Upconversion Nanoplatforms for Selective Biodetection, *Accounts of Chemical Research,* 50, 2017, pp. 32-40.

[15]. J. Zhao, Z. Lu, Y. Yin, C. McRae, J. A. Piper, J. M. Dawes, D. Jin, E. M. Goldys, Upconversion luminescence with tunable lifetime in $NaYF_4$: Yb, Er nanocrystals: role of nanocrystal size, *Nanoscale*, 5, 2013, pp. 944-952.

[16]. F. Wang, X. Liu, Upconversion multicolor fine-tuning: visible to near-infrared emission from lanthanide-doped $NaYF_4$ nanoparticles, *Journal of the American Chemical Society,* 130, 2008, pp. 5642-5643.

[17]. Y. Lu, J. Zhao, R. Zhang, Y. Liu, D. Liu, E. M. Goldys, X. Yang, P. Xi, A. Sunna, J. Lu, Tunable lifetime multiplexing using luminescent nanocrystals, *Nature Photonics*, 8, 2014, pp. 32-36.

[18]. F. Wang, R. Deng, J. Wang, Q. Wang, Y. Han, H. Zhu, X. Chen, X. Liu, Tuning upconversion through energy migration in core-shell nanoparticles, *Nature Materials,* 10, 2011, pp. 968-973.

[19]. H. H. Gorris, O. S. Wolfbeis, Photon-upconverting nanoparticles for optical encoding and multiplexing of cells, biomolecules, and microspheres, *Angewandte Chemie International Edition*, 52, 2013, pp. 3584-3600.

[20]. Y. Liu, M. Chen, T. Cao, Y. Sun, C. Li, Q. Liu, T. Yang, L. Yao, W. Feng, F. Li, A cyanine-modified nanosystem for in vivo upconversion luminescence bioimaging of methylmercury, *Journal of the American Chemical Society,* 135, 2013, pp. 9869-9876.

[21]. S. Wu, G. Han, D. J. Milliron, S. Aloni, V. Altoe, D. V. Talapin, B. E. Cohen, P. J. Schuck, Non-blinking and photostable upconverted luminescence from single lanthanide-doped nanocrystals, *Proceedings of the National Academy of Sciences,* 106, 2009, pp. 10917-10921.

[22]. J. Lai, B. P. Shah, Y. Zhang, L. Yang, K. -B. Lee, Real-time monitoring of ATP-responsive drug release using mesoporous-silica-coated multicolor upconversion nanoparticles, *ACS Nano*, 9, 2015, pp. 5234-5245.

[23]. H. Chen, J. Ren, Sensitive determination of chromium (VI) based on the inner filter effect of upconversion luminescent nanoparticles ($NaYF_4$: Yb^{3+}, Er^{3+}), *Talanta*, 99, 2012, pp. 404-408.
[24]. R. Ali, S. M. Saleh, R. J. Meier, H. A. Azab, I. I. Abdelgawad, O. S. Wolfbeis, Upconverting nanoparticle based optical sensor for carbon dioxide, *Sensors and Actuators B: Chemical*, 150, 2010, pp. 126-131.
[25]. R. J. Meier, J. M. Simbürger, T. Soukka, M. Schäferling, Background-free referenced luminescence sensing and imaging of pH using upconverting phosphors and color camera read-out, *Analytical Chemistry*, 86, 2014, pp. 5535-5540.
[26]. D. E. Achatz, R. J. Meier, L. H. Fischer, O. S. Wolfbeis, Luminescent sensing of oxygen using a quenchable probe and upconverting nanoparticles, *Angewandte Chemie International Edition*, 50, 2011, pp. 260-263.
[27]. L. Xie, Y. Qin, H.-Y. Chen, Polymeric optodes based on upconverting nanorods for fluorescent measurements of pH and metal ions in blood samples, *Analytical Chemistry*, 84, 2012, pp. 1969-1974.
[28]. L. Xie, Y. Qin, H. -Y. Chen, Direct fluorescent measurement of blood potassium with polymeric optical sensors based on upconverting nanomaterials, *Analytical Chemistry*, 85, 2013, pp. 2617-2622.
[29]. Y. -W. Zhang, X. Sun, R. Si, L. -P. You, C. -H. Yan, Single-crystalline and monodisperse LaF_3 triangular nanoplates from a single-source precursor, *Journal of the American Chemical Society*, 127, 2005, pp. 3260-3261.
[30]. Z. Li, Y. Zhang, An efficient and user-friendly method for the synthesis of hexagonal-phase $NaYF_4$: Yb, Er/Tm nanocrystals with controllable shape and upconversion fluorescence, *Nanotechnology*, 19, 2008, 345606.
[31]. X. Wang, J. Zhuang, Q. Peng, Y. Li, A general strategy for nanocrystal synthesis, *Nature*, 437, 2005, pp. 121-124.
[32]. F. Wang, D. K. Chatterjee, Z. Li, Y. Zhang, X. Fan, M. Wang, Synthesis of polyethylenimine/$NaYF_4$ nanoparticles with upconversion fluorescence, *Nanotechnology*, 17, 2006, p. 5786.
[33]. G. Yi, H. Lu, S. Zhao, Y. Ge, W. Yang, D. Chen, L. -H. Guo, Synthesis, characterization, and biological application of size-controlled nanocrystalline $NaYF_4$: Yb, Er infrared-to-visible up-conversion phosphors, *Nano Letters,* 4, 2004, pp. 2191-2196.
[34]. Z. Li, Y. Zhang, Monodisperse silica-coated polyvinylpyrrolidone/$NaYF_4$ nanocrystals with multicolor upconversion fluorescence emission, *Angewandte Chemie*, 118, 2006, pp. 7896-7899.
[35]. T. Zhang, J. Ge, Y. Hu, Y. Yin, A general approach for transferring hydrophobic nanocrystals into water, *Nano Letters*, 7, 2007, pp. 3203-3207.
[36]. A. Dong, X. Ye, J. Chen, Y. Kang, T. Gordon, J. M. Kikkawa, C. B. Murray, A generalized ligand-exchange strategy enabling sequential surface functionalization of colloidal nanocrystals, *Journal of the American Chemical Society*, 133, 2010, pp. 998-1006.

[37]. Z. Chen, H. Chen, H. Hu, M. Yu, F. Li, Q. Zhang, Z. Zhou, T. Yi, C. Huang, Versatile synthesis strategy for carboxylic acid-functionalized upconverting nanophosphors as biological labels, *Journal of the American Chemical Society,* 130, 2008, pp. 3023-3029.

[38]. F. Herranz, M. Morales, A. G. Roca, M. Desco, J. Ruiz-Cabello, A new method for the rapid synthesis of water stable superparamagnetic nanoparticles, *Chemistry-A European Journal,* 14, 2008, pp. 9126-9130.

[39]. H. P. Zhou, C. H. Xu, W. Sun, C. H. Yan, Clean and Flexible Modification Strategy for Carboxyl/Aldehyde-Functionalized Upconversion Nanoparticles and Their Optical Applications, *Advanced Functional Materials,* 19, 2009, pp. 3892-3900.

[40]. M. Wang, J. -L. Liu, Y. -X. Zhang, W. Hou, X. -L. Wu, S. -K. Xu, Two-phase solvothermal synthesis of rare-earth doped $NaYF_4$ upconversion fluorescent nanocrystals, *Materials Letters*, 63, 2009, pp. 325-327.

[41]. N. Bogdan, F. Vetrone, G. A. Ozin, J. A. Capobianco, Synthesis of ligand-free colloidally stable water dispersible brightly luminescent lanthanide-doped upconverting nanoparticles, *Nano Letters,* 11, 2011, pp. 835-840.

[42]. G. Jiang, J. Pichaandi, N. J. Johnson, R. D. Burke, F. C. van Veggel, An effective polymer cross-linking strategy to obtain stable dispersions of upconverting $NaYF_4$ nanoparticles in buffers and biological growth media for biolabeling applications, *Langmuir*, 28, 2012, pp. 3239-3247.

[43]. L. Cheng, K. Yang, S. Zhang, M. Shao, S. Lee, Z. Liu, Highly-sensitive multiplexed in vivo imaging using PEGylated upconversion nanoparticles, *Nano Research,* 3, 2010, pp. 722-732.

[44]. L. Wang, R. Yan, Z. Huo, L. Wang, J. Zeng, J. Bao, X. Wang, Q. Peng, Y. Li, Fluorescence resonant energy transfer biosensor based on upconversion-luminescent nanoparticles, *Angewandte Chemie International Edition*, 44, 2005, pp. 6054-6057.

[45]. C. Wang, L. Cheng, Y. Liu, X. Wang, X. Ma, Z. Deng, Y. Li, Z. Liu, Imaging-Guided Ph-Sensitive Photodynamic Therapy Using Charge Reversible Upconversion Nanoparticles under Near-Infrared Light, *Advanced Functional Materials*, 23, 2013, pp. 3077-3086.

[46]. J. -N. Liu, W. -B. Bu, J. -L. Shi, Silica coated upconversion nanoparticles: A versatile platform for the development of efficient theranostics, *Accounts of Chemical Research*, 48, 2015, pp. 1797-1805.

[47]. A. Sedlmeier, H. H. Gorris, Surface modification and characterization of photon-upconverting nanoparticles for bioanalytical applications, *Chemical Society Reviews*, 44, 2015, pp. 1526-1560.

[48]. M. Wang, G. Abbineni, A. Clevenger, C. Mao, S. Xu, Upconversion nanoparticles: synthesis, surface modification and biological applications, Nanomedicine: Nanotechnology, *Biology and Medicine*, 7, 2011, pp. 710-729.

[49]. J. Zhou, Z. Liu, F. Li, Upconversion nanophosphors for small-animal imaging, *Chemical Society Reviews,* 41, 2012, pp. 1323-1349.

[50]. J. Zhang, B. Li, L. Zhang, H. Jiang, An optical sensor for Cu (II) detection with upconverting luminescent nanoparticles as an excitation source, *Chemical Communications*, 48, 2012, pp. 4860-4862.
[51]. L. Yao, J. Zhou, J. Liu, W. Feng, F. Li, Iridium-Complex-Modified Upconversion Nanophosphors for Effective LRET Detection of Cyanide Anions in Pure Water, *Advanced Functional Materials*, 22, 2012, pp. 2667-2672.
[52]. Y. Ding, H. Zhu, X. Zhang, J. -J. Zhu, C. Burda, Rhodamine B derivative-functionalized upconversion nanoparticles for FRET-based Fe^{3+}-sensing, *Chemical Communications*, 49, 2013, pp. 7797-7799.
[53]. L. Yan, Y. -N. Chang, W. Yin, X. Liu, D. Xiao, G. Xing, L. Zhao, Z. Gu, Y. Zhao, Biocompatible and flexible graphene oxide/upconversion nanoparticle hybrid film for optical pH sensing, *Physical Chemistry Chemical Physics,* 16, 2014, pp. 1576-1582.
[54]. J. Peng, W. Xu, C. L. Teoh, S. Han, B. Kim, A. Samanta, J. C. Er, L. Wang, L. Yuan, X. Liu, High-efficiency in vitro and in vivo detection of Zn2+ by dye-assembled upconversion nanoparticles, *Journal of the American Chemical Society*, 137, 2015, pp. 2336-2342.
[55]. Q. Liu, Y. Sun, T. Yang, W. Feng, C. Li, F. Li, Sub-10 nm Hexagonal Lanthanide-Doped $NaLuF_4$ Upconversion Nanocrystals for Sensitive Bioimaging in Vivo, *Journal of the American Chemical Society*, 133, 2011, pp. 17122-17125.
[56]. W. Zou, C. Visser, J. A. Maduro, M. S. Pshenichnikov, J. C. Hummelen, Broadband dye-sensitized upconversion of near-infrared light, *Nature Photonics,* 6, 2012, pp. 560-564.
[57]. J. Lu, Y. Chen, D. Liu, W. Ren, Y. Lu, Y. Shi, J. Piper, I. Paulsen, D. Jin, One-step protein conjugation to upconversion nanoparticles, *Analytical Chemistry*, 87, 2015, pp. 10406-10413.
[58]. A. E. Guller, A. N. Generalova, E. V. Petersen, A. V. Nechaev, I. A. Trusova, N. N. Landyshev, A. Nadort, E. A. Grebenik, S. M. Deyev, A. B. Shekhter, Cytotoxicity and non-specific cellular uptake of bare and surface-modified upconversion nanoparticles in human skin cells, *Nano Research*, 8, 2015, pp. 1546-1562.
[59]. Z. Li, S. Lv, Y. Wang, S. Chen, Z. Liu, Construction of LRET-based nanoprobe using upconversion nanoparticles with confined emitters and bared surface as luminophore, *Journal of the American Chemical Society*, 137, 2015, pp. 3421-3427.
[60]. M. Kumar, P. Zhang, Highly sensitive and selective label-free optical detection of mercuric ions using photon upconverting nanoparticles, *Biosensors and Bioelectronics*, 25, 2010, pp. 2431-2435.
[61]. M. Kumar, P. Zhang, Highly sensitive and selective label-free optical detection of DNA hybridization based on photon upconverting nanoparticles, *Langmuir*, 25, 2009, pp. 6024-6027.
[62]. P. Alonso-Cristobal, P. Vilela, A. El-Sagheer, E. Lopez-Cabarcos, T. Brown, O. Muskens, J. Rubio-Retama, A. Kanaras, Highly sensitive

DNA sensor based on upconversion nanoparticles and graphene oxide, *ACS Applied Materials & Interfaces*, 7, 2015, pp. 12422-12429.

[63]. Y. Wang, L. Bao, Z. Liu, D. -W. Pang, Aptamer biosensor based on fluorescence resonance energy transfer from upconverting phosphors to carbon nanoparticles for thrombin detection in human plasma, *Analytical Chemistry*, 83, 2011, pp. 8130-8137.

[64]. L. Liu, B. Li, R. Qin, H. Zhao, X. Ren, Z. Su, Synthesis and characterization of new bifunctional nanocomposites possessing upconversion and oxygen-sensing properties, *Nanotechnology*, 21, 2010, 285701.

[65]. S. Liu, L. Zhang, T. Yang, H. Yang, K. Y. Zhang, X. Zhao, W. Lv, Q. Yu, X. Zhang, Q. Zhao, Development of upconversion luminescent probe for ratiometric sensing and bioimaging of hydrogen sulfide, *ACS Applied Materials & Interfaces*, 6, 2014, pp. 11013-11017.

[66]. C. Li, J. Liu, S. Alonso, F. Li, Y. Zhang, Upconversion nanoparticles for sensitive and in-depth detection of Cu^{2+} ions, *Nanoscale*, 4, 2012, pp. 6065-6071.

[67]. R. Han, H. Yi, J. Shi, Z. Liu, H. Wang, Y. Hou, Y. Wang, pH-Responsive drug release and NIR-triggered singlet oxygen generation based on a multifunctional core–shell–shell structure, *Physical Chemistry Chemical Physics*, 18, 2016, pp. 25497-25503.

[68]. J. Liu, Y. Liu, W. Bu, J. Bu, Y. Sun, J. Du, J. Shi, Ultrasensitive nanosensors based on upconversion nanoparticles for selective hypoxia imaging in vivo upon near-infrared excitation, *Journal of the American Chemical Society*, 136, 2014, pp. 9701-9709.

[69]. L. Zhao, J. Peng, M. Chen, Y. Liu, L. Yao, W. Feng, F. Li, Yolk-shell upconversion nanocomposites for LRET sensing of cysteine/homocysteine, *ACS Applied Materials & Interfaces*, 6, 2014, pp. 11190-11197.

[70]. H. Li, L. Wang, $NaYF_4$: Yb^{3+}/Er^{3+} nanoparticle-based upconversion luminescence resonance energy transfer sensor for mercury (II) quantification, *Analyst*, 138, 2013, pp. 1589-1595.

[71]. J. Liu, Y. Liu, Q. Liu, C. Li, L. Sun, F. Li, Iridium (III) complex-coated nanosystem for ratiometric upconversion luminescence bioimaging of cyanide anions, *Journal of the American Chemical Society*, 133, 2011, pp. 15276-15279.

[72]. P. Zhang, S. Rogelj, K. Nguyen, D. Wheeler, Design of a highly sensitive and specific nucleotide sensor based on photon upconverting particles, *Journal of the American Chemical Society*, 128, 2006, pp. 12410-12411.

[73]. F. Zhou, U. J. Krull, Spectrally matched duplexed nucleic acid bioassay using two-colors from a single form of upconversion nanoparticle, *Analytical Chemistry*, 86, 2014, pp. 10932-10939.

[74]. M. Kumar, Y. Guo, P. Zhang, Highly sensitive and selective oligonucleotide sensor for sickle cell disease gene using photon upconverting nanoparticles, *Biosensors and Bioelectronics*, 24, 2009, pp. 1522-1526.

[75]. F. Yuan, H. Chen, J. Xu, Y. Zhang, Y. Wu, L. Wang, Aptamer-Based Luminescence Energy Transfer from Near-Infrared-to-Near-Infrared Upconverting Nanoparticles to Gold Nanorods and Its Application for the Detection of Thrombin, *Chemistry-A European Journal*, 20, 2014, pp. 2888-2894.

[76]. H. Chen, F. Yuan, S. Wang, J. Xu, Y. Zhang, L. Wang, Aptamer-based sensing for thrombin in red region via fluorescence resonant energy transfer between $NaYF_4$: Yb, Er upconversion nanoparticles and gold nanorods, *Biosensors and Bioelectronics*, 48, 2013, pp. 19-25.

[77]. S. Xu, B. Dong, D. Zhou, Z. Yin, S. Cui, W. Xu, B. Chen, H. Song, Paper-based upconversion fluorescence resonance energy transfer biosensor for sensitive detection of multiple cancer biomarkers, *Scientific Reports*, 6, 2016, p. 23406.

[78]. E.-J. Jo, H. Mun, M.-G. Kim, Homogeneous immunosensor based on luminescence resonance energy transfer for glycated hemoglobin detection using upconversion nanoparticles, *Analytical Chemistry*, 88, 2016, pp. 2742-2746.

[79]. C. Liu, Z. Wang, H. Jia, Z. Li, Efficient fluorescence resonance energy transfer between upconversion nanophosphors and graphene oxide: a highly sensitive biosensing platform, *Chemical Communications*, 47, 2011, pp. 4661-4663.

[80]. C. Zhang, Y. Yuan, S. Zhang, Y. Wang, Z. Liu, Biosensing platform based on fluorescence resonance energy transfer from upconverting nanocrystals to graphene oxide, *Angewandte Chemie International Edition*, 50, 2011, pp. 6851-6854.

[81]. R. Deng, X. Xie, M. Vendrell, Y.-T. Chang, X. Liu, Intracellular glutathione detection using MnO_2-nanosheet-modified upconversion nanoparticles, *Journal of the American Chemical Society*, 133, 2011, pp. 20168-20171.

[82]. Y. Wang, P. Shen, C. Li, Y. Wang, Z. Liu, Upconversion fluorescence resonance energy transfer based biosensor for ultrasensitive detection of matrix metalloproteinase-2 in blood, *Analytical Chemistry*, 84, 2012, pp. 1466-1473.

[83]. S. Wu, N. Duan, X. Ma, Y. Xia, H. Wang, Z. Wang, Q. Zhang, Multiplexed fluorescence resonance energy transfer aptasensor between upconversion nanoparticles and graphene oxide for the simultaneous determination of mycotoxins, *Analytical Chemistry*, 84, 2012, pp. 6263-6270.

[84]. S. Jiang, Y. Zhang, Upconversion nanoparticle-based FRET system for study of siRNA in live cells, *Langmuir*, 26, 2010, pp. 6689-6694.

[85]. S. Li, L. Xu, W. Ma, X. Wu, M. Sun, H. Kuang, L. Wang, N. A. Kotov, C. Xu, Dual-mode ultrasensitive quantification of microRNA in living cells by chiroplasmonic nanopyramids self-assembled from gold and upconversion nanoparticles, *Journal of the American Chemical Society*, 138, 2016, pp. 306-312.

[86]. P. Vilela, A. El-Sagheer, T. M. Millar, T. Brown, O. L. Muskens, A. G. Kanaras, Graphene Oxide-Upconversion Nanoparticle Based

Optical Sensors for Targeted Detection of mRNA Biomarkers Present in Alzheimer's Disease and Prostate Cancer, *ACS Sensors*, 2, 2017, pp. 52-56.

[87]. M. Wang, W. Hou, C. -C. Mi, W. -X. Wang, Z. -R. Xu, H. -H. Teng, C.-B. Mao, S. -K. Xu, Immunoassay of goat antihuman immunoglobulin G antibody based on luminescence resonance energy transfer between near-infrared responsive $NaYF_4$: Yb, Er upconversion fluorescent nanoparticles and gold nanoparticles, *Analytical Chemistry,* 81, 2009, pp. 8783-8789.

[88]. H. S. Mader, O. S. Wolfbeis, Optical ammonia sensor based on upconverting luminescent nanoparticles, *Analytical Chemistry*, 82, 2010, pp. 5002-5004.

[89]. H. Chen, H. Li, J. -M. Lin, Determination of ammonia in water based on chemiluminescence resonance energy transfer between peroxymonocarbonate and branched $NaYF_4$: Yb^{3+}/Er^{3+} nanoparticles, *Analytical Chemistry,* 84, 2012, pp. 8871-8879.